NWC TP 7032

Application of Maximum Entropy Analysis to ISAR Imagery and Spurious Scatterer Location in Anechoic Chambers

by
Brett Borden
Research Department

OCTOBER 1989

NAVAL WEAPONS CENTER
CHINA LAKE, CA 93555-6001

Approved for public release; distribution is unlimited.

Naval Weapons Center

FOREWORD

The research described in this report was performed in fiscal years 1988 and 1989 as part of an effort to improve imaging resolution from incomplete and noisy data. Maximum entropy methods are known to be optimal in such situations; however, partly because they are perceived to be "difficult to understand," they have not been well used. It is hoped that this final report will help to remedy this situation by demonstrating how effective the method can be in several applied imaging problems. This effort was supported by the Office of Naval Research, Code 1247.

Gary A. Hewer has reviewed this report for technical accuracy.

Approved by
R. L. DERR, *Head*
Research Department
25 September 1989

Under authority of
D. W. COOK
Capt., U.S. Navy
Commander

Released for publication by
G. R. SCHIEFER
Technical Director

NWC Technical Publication 7032

Published by . . . . Technical Information Department
Collation . . . . Cover, 8 leaves
First printing . . . . 90 copies

REPORT DOCUMENTATION PAGE

Form Approved
OMB No. 0704-0188

1. AGENCY USE ONLY *(Leave blank)*

2. REPORT DATE
Oct 89

3. REPORT TYPE AND DATES COVERED
Final, Oct 87 to Sep 89

4. TITLE AND SUBTITLE
APPLICATION OF MAXIMUM ENTROPY ANALYSIS TO ISAR IMAGERY AND SPURIOUS SCATTERER LOCATION IN ANECHOIC CHAMBERS

5. FUNDING NUMBERS
PE 61153N
PR R01411
TA R01411
WU 909033

6. AUTHOR(S)
Brett Borden

7. PERFORMING ORGANIZATION NAME(S) AND ADDRESS(ES)
Naval Weapons Center
China Lake, CA 93555-6001

8. PERFORMING ORGANIZATION REPORT NUMBER
NWC TP 7032

9. SPONSORING/MONITORING AGENCY NAME(S) AND ADDRESS(ES)
Office of Naval Research
Arlington, VA 22217

10. SPONSORING/MONITORING AGENCY REPORT NUMBER

11. SUPPLEMENTARY NOTES

12a. DISTRIBUTION/AVAILABILITY STATEMENT
A Statement; public release; distribution unlimited

12b. DISTRIBUTION CODE

13. ABSTRACT *(Maximum 200 words)*

(U) The maximum entropy method is applied to two problems, both of which require high resolution imaging from incomplete data. For systems of scatterers with limited extent, the scattered field generally spans the entire "frequency" domain, and the data are usually available only from a finite region of this domain. Furthermore, often only the magnitude of the scattered field can be measured and the phase information is lost. We examine first the case where the phase is known, using a method originally developed for radio astronomy imaging, and apply the results to the problem of inverse synthetic aperture radar (ISAR) imagery. Then we show how these results can be modified for the case where phase information is missing and apply the method to the problem of "hot spot" location in anechoic chambers. Comparisons are made with standard (Fourier) methods.

14. SUBJECT TERMS
Maximum entropy, Imaging, ISAR

15. NUMBER OF PAGES
13

16. PRICE CODE

17. SECURITY CLASSIFICATION OF REPORT	18. SECURITY CLASSIFICATION OF THIS PAGE	19. SECURITY CLASSIFICATION OF ABSTRACT	20. LIMITATION OF ABSTRACT
UNCLASSIFIED	UNCLASSIFIED	UNCLASSIFIED	UL

INTRODUCTION

In the weak scatterer approximation, the scattered field response E, resulting from a harmonic excitation of a "target," can be modeled by a superposition of plane waves

$$E(\mathbf{k}) = \int_D \varepsilon(\mathbf{r})\, e^{i\mathbf{k}\cdot\mathbf{r}}\, d^3r \quad , \tag{1}$$

where $\varepsilon(\mathbf{r})$ is defined by the local scatterer strength at the position $\mathbf{r}$, $\mathbf{k}$ is the propagation vector with magnitude $2\pi/\lambda$, and the integral is over the support of the target D. (The $\exp(-i\omega t)$ time dependence has been suppressed.)

In general, when D is finite, $E(\mathbf{k})$ spans k-space and Equation 1 usually cannot be uniquely inverted to obtain the $\varepsilon(\mathbf{r})$ from a limited (finite and discrete) set of scattered field measurements. Moreover, the effects of making assumptions about the *unknown* data (for example, that they are identically zero) distort the image $\varepsilon(\mathbf{r})$. However, since D is already space-limited, this equation can be used as a governing equation determining the $\varepsilon'(\mathbf{r})$ that is consistent with the data; this can be done by least-squares comparison between the predicted and observed portion of the scattered field (Reference 1).

In principle, when the data are noise-free and a solution to Equation 1 exists, this method leads to an unambiguous determination of $\varepsilon(\mathbf{r}) = \varepsilon'(\mathbf{r})$. But, when we account for the inevitable noise in the measured data, we find ourselves back to "best guessing" $\varepsilon(\mathbf{r})$ from a *set* of allowed images $\{\varepsilon'(\mathbf{r})\}$.

In the following section, we briefly review the principle of maximum entropy (maxent) and show how it can be used to select the *least-biased* image from the set of images consistent with the measured data and noise. Then we apply the method to the problems of (1) inverse synthetic aperture radar (ISAR) imagery, for which the phase part of the scattered field is known and (2) hot-spot location in anechoic chambers, for which the phase is not known.

MAXIMUM ENTROPY SOLUTION

The detailed foundations of the maximum entropy principle have been well developed elsewhere; we shall proceed without *ab initio* motivation (cf., References 2 through 8). The measured field data will be of the form

$$M_m = E_m + \alpha_m \sigma_m \quad , \quad m = 1, \ldots , P \quad ,$$

where σ_m is the standard deviation of the measurement and α_m is assumed to be a mean zero (usually Gaussian) random variable of unit variance. Suppose $\varepsilon'(\mathbf{r})$ is a trial solution to (1) and E' is the associated trial field, which is to be compared with measured field data M. The logarithm of the likelihood of observing a particular data set from a given $\varepsilon'(\mathbf{r})$ gives the χ^2 test in the form

$$\chi^2 = \sum_{m=1}^{P} (M_m - E'_m)^2 / \sigma_m^2 \quad .$$

This χ^2 test can be used to define feasible solutions. In particular, when the data are many, the expectation of χ^2 approaches P and our feasibility criterion becomes (Reference 9)

$$\sum_{m=1}^{P} (M_m - E'_m)^2 / \sigma_m^2 = P \quad . \tag{2}$$

The maximum entropy method allows us to select from the set of all $\varepsilon'(\mathbf{r})$ satisfying Equation 2, the one that is least biased based on the data (Reference 2). To accomplish this, we form the Shannon-Jaynes entropy

$$S(\varepsilon) \equiv - \int p\,(\mathbf{r}')\,\ln[p(\mathbf{r}')]\,dV' \quad ,$$

where

$$p\,(\mathbf{r}') \equiv \frac{|\varepsilon(\mathbf{r})|}{\int |\varepsilon(\mathbf{r}')|\;dV'} \quad . \tag{3}$$

The distribution $\varepsilon(\mathbf{r})$, which maximizes $S(\varepsilon)$ subject to the constraint of Equation 2, is the maximum entropy solution. This is also the distribution with the greatest degeneracy (Reference 3).

If we discretize Equations 1 and 3 by introducing the approximation $\varepsilon_n \equiv \varepsilon(\mathbf{r})\,\delta(\mathbf{r} - \mathbf{r}_n)$, $n = 1,\ldots,N$, then the problem becomes one of constrained optimization over the variables ε_n. This may be treated by introducing the Lagrange multiplier λ so that we seek solutions to the simultaneous system of equations:

$$\nabla_\varepsilon \left[-\sum_{n=1}^{N} p_n \ln (p_n) \right] = \lambda \nabla_\varepsilon \left[P - \sum_{m=1}^{P} (M_m - E_m)^2/\sigma_m^2 \right] \tag{4}$$

$$\sum_{m=1}^{P} (M_m - E_m)^2/\sigma_m^2 = P \quad ,$$

where

$$p_n = \frac{|\varepsilon_n|}{\sum_{i=1}^{N} |\varepsilon_i|}$$

and E_m is determined using

$$E_m = \sum_{n=1}^{N} \varepsilon_n \exp(i\mathbf{k}_m \cdot \mathbf{r}_n) \quad .$$

(∇_ε denotes the vector operator $\nabla_\varepsilon = \sum_i u_i \, \partial/\partial\varepsilon_i$, where $\{u_i\}$ is an independent basis set.)

The resulting N+1 equations are nonlinear in ε_n and in general must be solved iteratively.

SAMPLE ISAR APPLICATION

For a target with rotational position $\theta(t)$ in the far-field of the transmitter/receiver, Equation 1 becomes (Reference 10)

$$E(k,\theta) = \int_D \varepsilon(x,y) \exp[ik(y \cos\theta - x \sin\theta)] \, dx \, dy \quad ,$$

where $k = 2 \times 2\pi/\lambda$ (the factor of 2 accounts for the two-way travel distance from transmitter to co-located receiver) and now $\varepsilon(x,y)$ represents the integrated contribution of the scatterer strengths along the axis of rotation. If we set $\xi = 4\pi \sin(\theta)/\lambda$ and $\psi = -4\pi \cos(\theta)/\lambda$, then this equation, in its discrete form, becomes

$$E_{lm} = \sum_{r=1}^{R} \sum_{s=1}^{S} \varepsilon_{rs} \exp[-i(x_r \xi_l + y_s \psi_m)] \quad . \tag{5}$$

With this indexing scheme, Equation 4 yields

$$\varepsilon_{rs} = \exp(\rho + 2\lambda\eta\gamma_{rs}) \quad r = 1, \ldots, R \, ; \, s = 1, \ldots, S$$

and

$$\sum_{l=1}^{L} \sum_{m=1}^{M} | M_{lm} - E_{lm} |^2 / \sigma_{lm}^2 = LM \quad ,$$

where

$$\eta \equiv \sum_{r=1}^{R} \sum_{s=1}^{S} \varepsilon_{rs} \quad ,$$

$$\rho \equiv \sum_{r=1}^{R} \sum_{s=1}^{S} \varepsilon_{rs} \ln(\varepsilon_{rs}) \quad ,$$

$$\gamma_{rs} \equiv \mathrm{Re}\left\{ \sum_{l=1}^{L} \sum_{m=1}^{M} (M_{lm} - E_{lm})/\sigma_{lm}^2 \exp[i(x_r \xi_l + y_s \psi_m)] \right\} \quad ,$$

and E_{lm} are determined by Equation 5.

All but the last of these equations are of the form $\varepsilon_{rs} = f_{rs}(\varepsilon)$ and thus can be solved by successive substitution (Reference 11) (i.e., if $\varepsilon^{(i)}$ denotes the ith iterate, then we set $\varepsilon_{rs}{}^{(i+1)} = f_{rs}[\varepsilon^{(i)}]$). Following an observation by Lieu, we set $\lambda = 1/LM$ (Reference 12). For regularly spaced data, both E_{lm} and γ_{rs} can be determined by fast-Fourier transform techniques, and the entire iterative process converges quite rapidly (typically, within 50 iterations).

Figure 1 displays sample results of this maximum entropy reconstruction. For comparison purposes, we have included also the reconstruction obtained by windowing the data and inverse Fourier transforming the result. The target consisted of two small aluminum dihedrals mounted on a rotating pedestal. Data were collected using 101 frequencies equally spaced from 45 to 75 gigahertz and discretized to 32 angles from -2 to 2 degrees in aspect. The plots are logarithmic, and the maximum entropy reconstruction displays the result of "ringing," or multiple reflections from each dihedral.

Comparison between the two reconstructions demonstrates the utility in the maxent approach. Not only was resolution significantly increased, but the sidelobes present in the inverse Fourier transform result were completely eliminated in the maximum entropy image.

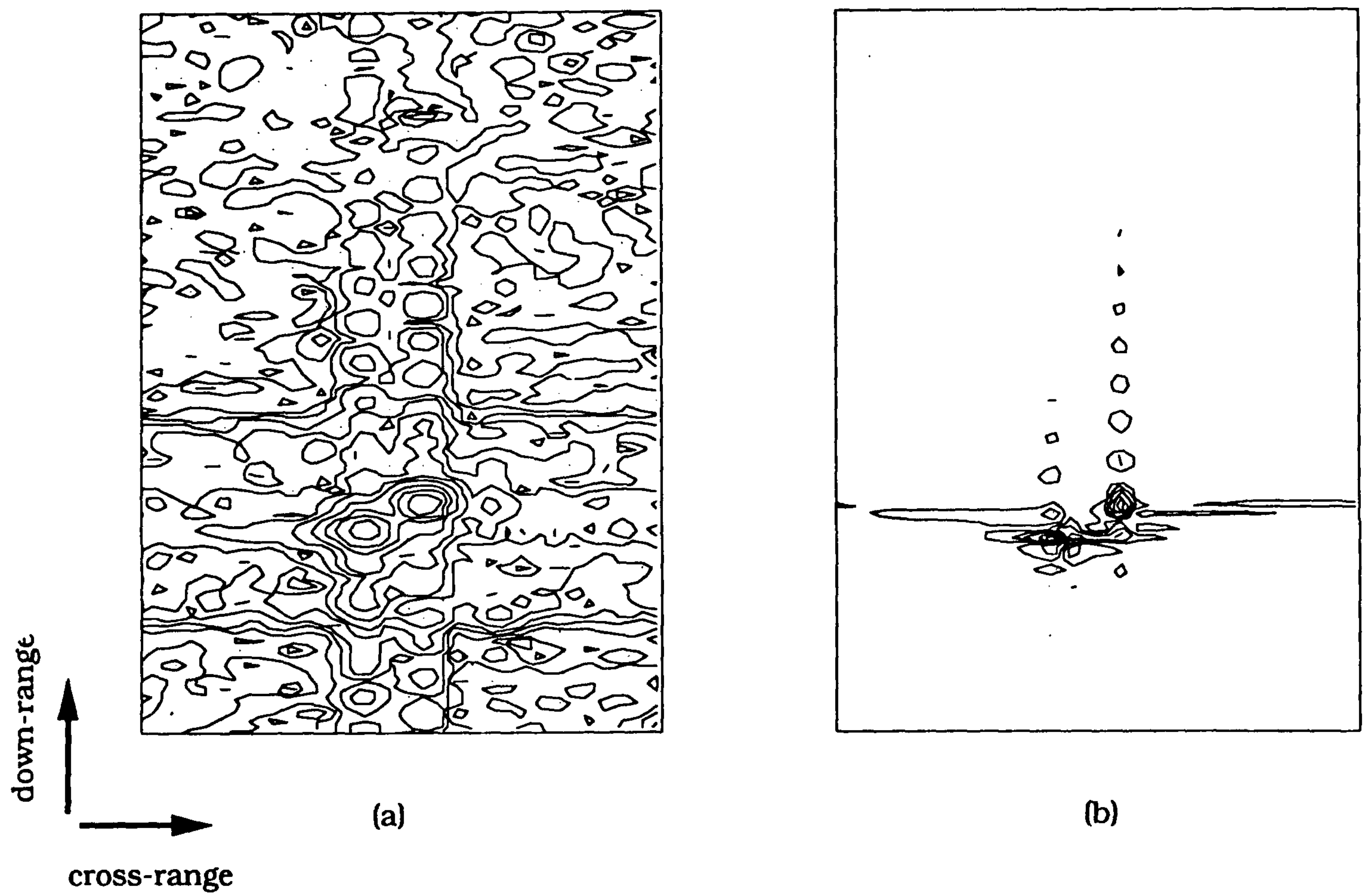

FIGURE 1. Sample Results: Two Dihedrals Imaged Using Ordinary Fourier Methods (a) and Maximum Entropy Methods (b). Plots are logarithmic. The multiple "down range" images are the result of repeated target "ringing."

PHASELESS FOURIER DATA—ANECHOIC CHAMBER DIAGNOSTICS

The use of anechoic chambers for the testing and evaluation of radiating systems has become commonplace in recent years. These chambers allow for a level of parameter control and noise isolation unparalleled in corresponding free-space experiments. However, it has long been known that actual chambers cannot be expected to work perfectly and do not always correctly model free-space. There are usually spurious reflections from the imperfectly absorbing walls. Typically, these background reflections are small—less than -30 decibels of the desired signal. But frequently these unwanted reflections worsen as the chamber ages, and occasionally they become significant enough to ruin the usefulness of the chamber.

Considerable effort has been devoted to this problem, and various schemes have been proposed in the past to characterize anechoic chambers and to try to correct for their inherent limitations (cf., References 13 through 19). Mostly, these schemes have been *ad hoc* and ambiguous, attempting to simply assign a figure of merit to a chamber based on comparison between intensity measurements and their predicted (free-space) values. In some cases, ray-tracing methods have been used to isolate specular effects in the scattered field. While the techniques of measuring the field intensity at various locations within the chamber have been well developed (Reference 15), little in the way of *systematic* determination of the location of the background scatterers has been attempted. For many applications, the effort may be unwarranted. However, for situations in which the defects may be corrected, the location problem is quite important.

The antenna-pattern comparison (APC) technique or the voltage standing-wave ratio (VSWR) technique allows for the determination of the ratio of the scattered-to-incident-field magnitudes at various locations within the chamber. Without loss of generality, we may take the incident field to have unit magnitude and therefore the measured data will be of the form

$$M_m = |E_m|^2 + \alpha_m \sigma_m \quad .$$

The allowed-image test is now

$$\sum_{m=1}^{P} (M_m - |E_m|^2)^2/\sigma_m^2 = P \quad ,$$

where E_m is calculated from Equation 1 for each trial image. (The remainder of Equation 4 must be similarly modified.) All other results follow as before.

Computer-synthesized data were constructed for "known" configurations of spurious scatterers. These data consisted of intensity ratios at random locations within the chamber with additive Gaussian noise and are intended to represent the kind of measurements that can be made by VSWR techniques. The amount of noise was set by choosing $\sigma_m = \sigma$ to be a fraction of $\varepsilon_{max} \equiv \max\{\varepsilon_n\}$. Values of $\sigma/\varepsilon_{max} = 0.001$ to 0.05 appear to be consistent with existing measurement capabilities (References 18, 20, 21).

The data were used to exercise the algorithm, and the resulting reconstruction was compared with the known scatterer distribution to test for accuracy. Figure 2 illustrates typical results for a cubical test chamber. For this reconstruction, 30 measurements were "made" at random locations with the noise level set at $\sigma = 0.001\,\varepsilon_{max}$. The resolution of this reconstruction was established by dividing the walls into 500 equal elements.

The maximum entropy method is known to be very sensitive to noise. Our reconstructions gave "good" results for σ/ε_{max} up to $\approx 1\%$ and "useful" results for σ/ε_{max} up to $\approx 5\%$. Beyond that level, too little information was provided by the reconstruction to accurately locate the background scatterers.

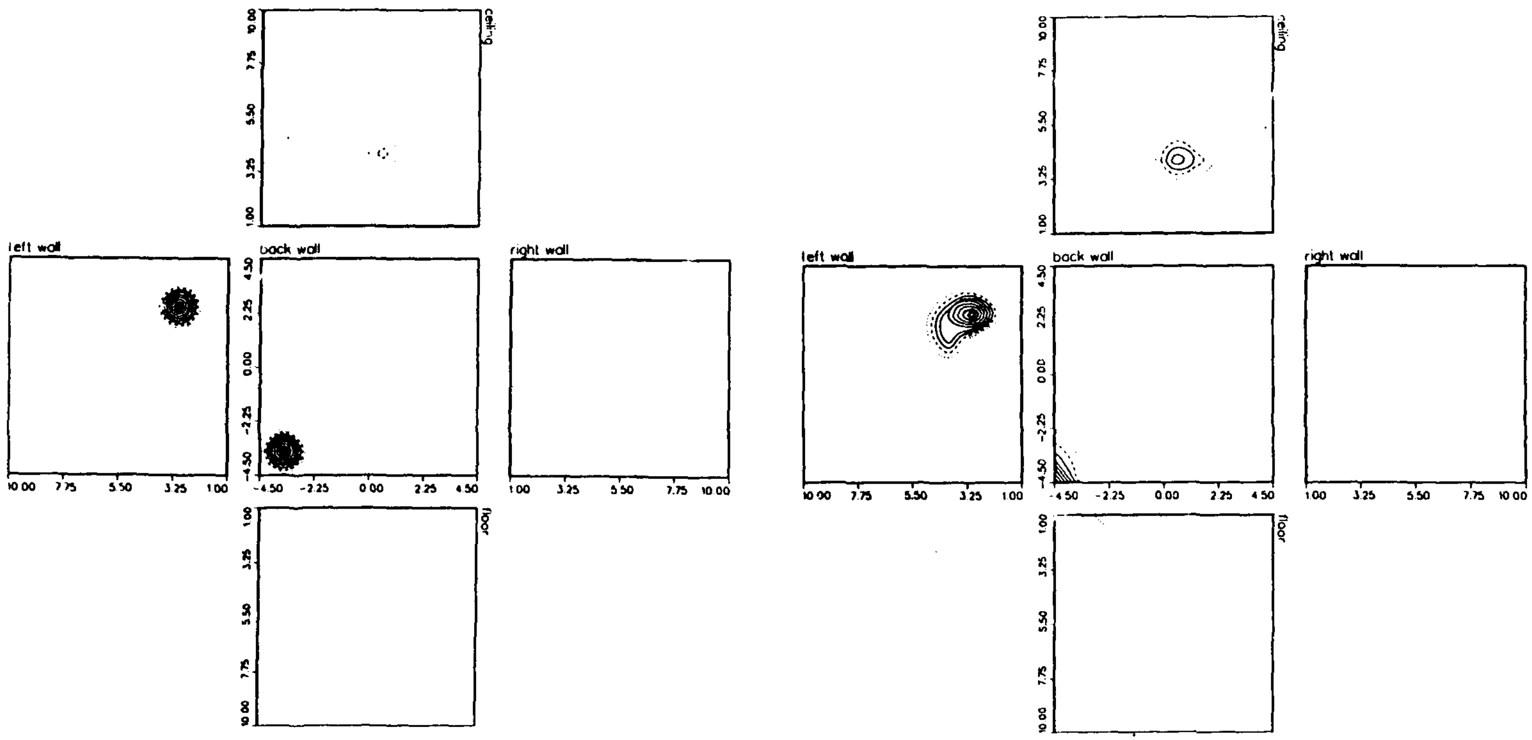

(a) (b)

FIGURE 2. Sample Reconstruction Results: (a) Actual Distribution of Background Scatterers and (b) Reconstruction Based on 30 Simulated VSWR Measurements From Random Locations Within the Chamber. Additive Gaussian noise was included using $\sigma = 0.001\ \varepsilon_{max}$.

CONCLUSION

The maximum entropy method has been applied to the problem of image reconstruction from both ordinary and phaseless Fourier data for which the standard deviation of the additive noise can be estimated and is small. For small data sets, the results are unambiguous in the sense that no additional information about the unmeasured data are assumed. For this reason, the reconstructions are superior to their usual Fourier-based counterparts.

The quality of the reconstructions comes with a price. Our implementation of the derived algorithms typically ran more than 100 times slower than simple Fourier inversion. Because of the multiple iterations required, it is doubtful that significant improvement of this figure can be accomplished. However, in situations where speed is not the driving concern. the quality of the results may warrant the extra effort.

REFERENCES

1. R. W. Gerchberg. "Super-Resolution Through Error Energy Reduction," *Opt. Acta*, Vol. 21 (1974), pp. 709-20.

2. R. K. Bryan and J. Skilling. "Maximum Entropy Image Reconstruction From Phaseless Fourier Data," *Ibid.*, Vol. 33 (1986), pp. 287-99.

3. E. T. Jaynes. "Information Theory and Statistical Mechanics," *Phys. Rev.*, Vol. 106 (1957), pp. 620-30.

4. ------. "Information Theory and Statistical Mechanics. II," *Ibid.*, Vol. 108 (1957), pp. 171-90.

5. ------. "On the Rationale of Maximum-Entropy Methods," *IEEE Proc.*, Vol. 70 (1982), pp. 939-52.

6. S. J. Wernecke and L. R. D'Addario. "Maximum Entropy Image Reconstruction," *IEEE Trans. Computers*, Vol. C26 (1977), pp. 351-64.

7. G. Bricogne. "Maximum Entropy and the Foundations of Direct Methods," *Acta Cryst.*, Vol. A40 (1984), pp. 410-45.

8. A. K. Livesey and J. Skilling. "Maximum Entropy Theory," *Ibid.*, Vol. A41 (1985), pp. 113-22.

9. S. F. Gull and G. J. Daniell. "Image Reconstruction From Incomplete and Noisy Data," *Nature*, Vol. 272 (1978), pp. 686-90.

10. D. L. Mensa. *High Resolution Radar Imaging*. Dedham, Mass., Artech House, Inc., 1981.

11. B. Carnahan, H. A. Luther, and J. O. Wilkes. *Applied Numerical Methods*. New York, Wiley, 1969.

12. R. Lieu. "The Maximum Entropy Configuration in the Case of Randomly Fluctuating Constraints," *J. Phys. A: Math. Gen.*, Vol. 22 (1989), pp. L483-L488.

13. E. F. Buckley. "Outline of Evaluation Procedures for Microwave Anechoic Chambers," *Microwave J.* (August 1963), pp. 69-75.

14. E. F. Buckley. "Design and Performance of Modern Microwave Anechoic Chambers for Antenna Measurements," *Electron. Components* (December 1965), pp. 1119-26.

15. J. Appel-Hansen. "Reflectivity Level of Radio Anechoic Chambers," *IEEE Trans. Antennas Propag.*, Vol. 21 (1973), pp. 490-98.

16. ------. "Precision Measurement of Backscattering Cross-Sections as a Function of Frequency," *IEEE Trans. Instrum. Meas.*, Vol. 25 (1976), pp. 363-70.

17. L. A. Robinson. "Design of Anechoic Chambers for Antenna and Radar-Cross-Section Measurements," ONR Contract N00014-81-K-0182 (NR 088-094), SRI Project 2495, Technical Report 2, SRI International, Menlo Park, Calif., 1982.

18. R. G. Fitzgerrel. "Using Free-Space Transmissi Loss for Evaluating Anechoic Chamber Performance," *IEEE Trans. Electromagn. Compat.*, Vol. 24 (1982), pp. 356-58.

19. E. N. Clouston, P. A. Langsford, and S. Evans. "Measurement of Anechoic Chamber Reflections by Time-Domain Techniques," *IEEE Proc.*, Vol. 135 (1988), pp. 93-97.

20. S. Tofani, L. Anglesio, G. Agnesod, and P. Ossola. "Electromagnetic Standard Fields: Generation and Accuracy Levels from 100 KHz to 990 MHz," *IEEE Trans. Microwave Theory Tech.*, Vol. 34 (1986), pp. 832-35.

21. M. Kanda, E. B. Larsen, M. Borsero, P. G. Galliano, I. Yokoshima, and N. S. Nahman. "Standards for Electromagnetic Field Measurements," *Proc. IEEE*, Vol. 74 (1986), pp. 120-28.

INITIAL DISTRIBUTION

4 Naval Air Systems Command
  AIR-5004 (2)
  AIR-933B (1)
  AIR-933E, D. Glista (1)
4 Chief of Naval Research
  J. Cauffman (1)
  Dr. K. Davis (1)
  Dr. R. Madan (1)
  J. Smith (1)
3 Naval Sea Systems Command
  C. E. Jedrey (1)
  Technical Library (2)
1 Commander in Chief, U. S. Pacific Fleet, Pearl Harbor (Code 325)
1 Commander, Third Fleet, San Francisco
1 Commander, Seventh Fleet, San Francisco
2 Naval Academy, Annapolis (Director of Research)
2 Naval Air Development Center, Warminster
  Code 3022, Dr. O. Kessler (1)
  Technical Library (1)
3 Naval Ocean Systems Center, San Diego
  P. Hansen (1)
  C. Ramstadt (1)
  Technical Library (1)
2 Naval Postgraduate School, Monterey, CA
  Dr. M. A. Morgan (1)
  Technical Library (1)
5 Naval Research Laboratory
  Code 7500, Dr. J. R. Davis (1)
  Code 7550
    D. Himes (1)
    L. Wagner (1)
  Dr. A. Jordan (1)
  Technical Library (1)
1 Naval War College, Newport
1 Air Force Intelligence Agency, Bolling Air Force Base (AFIA/INTAW, Maj. R. Esaw)
12 Defense Technical Information Center, Alexandria
1 A. J. Devaney Associates, Ridgefield, CT (Dr. A. J. Devaney)
1 AVCO Systems Textron, Wilmington, MA (Dr. R. L. Fante)
1 General Dynamics Corporation, San Diego, CA (Dr. C. P. Tricoles)
1 Hudson Institute, Incorporated, Center for Naval Analyses, Alexandria, VA (Technical Library)
1 Institute for Defense Analyses, Alexandria, VA (Dr. I. Kay)
2 Massachusettes Institute of Technology, Lincoln Laboratory, Lexington, MA
  Dr. R. M. Barnes (1)
  Dr. G. Morse (1)
1 Michigan State University, East Lansing, MI (Prof. K. M. Chen)
1 Ohio State University, Columbus, OH (Dr. E. Walton)
1 Purdue University, West Lafayette, IN (Prof. V. H. Weston)
1 University of California, Berkeley, CA (Prof. E. A. Grunbaum)
1 University of Illinois, Chicago, IL (Dr.W. Boerner)
1 University of Illinois, Urbana, IL (Prof. R. Mittra)
2 University of Pennsylvania, Philadelphia, PA
  Prof. N. Farhat (1)
  Dr. B. Steinberg (1)